NRC Research Press

ARTICLE

Physiological focus on the erythropoietin–hepcidin–ferroportin axis

María Cecilia D'Anna and Marta Elena Roque

Abstract: To analyze the interconnection between erythropoiesis and iron metabolism, one of the issues raised in this study was to know iron bioavailability under physiopathological conditions. Our aim was to understand the functional axis response composed of erythropoietin (Epo)—hepcidin—ferroportin (FPN), when 2 dysfunctional states coexist, using an animal model of iron overload followed by hypoxia. FPN and prohepcidin were assessed by immunohistochemistry using rabbit anti-mouse FPN polyclonal and prohepcidin monoclonal antibodies. Goat-labeled polymer – horseradish peroxidase anti-rabbit EnVision + System (DAB) was used as the secondary antibody. Epo levels were measured by ELISA. Tissue iron was studied by Prussian blue iron staining. Erythropoietic response was assessed using conventional hematological tests. Iron overload increased prohepcidin that remained high in hypoxia, coexisting with high levels of Epo in hypoxia, with or without iron overload. In hypoxia, FPN was clearly evident in reticuloendothelial macrophages, more than in hypoxia with iron overload. Interestingly, duodenal FPN was clearly identified on the basolateral membrane in hypoxia, with or without iron overload. Our data indicate that 2 signals could induce the cell-specific response as follows: (*i*) iron signal, induced prohepcidin, which reduced reticuloendothelial FPN and reduced iron availability; and (*ii*) hypoxia signal, stimulated Epo, which affected iron absorption by stabilizing duodenal FPN and allowed iron supply to erythropoiesis independently of store size.

Key words: ferroportin, prohepcidin, erythropoietin, iron, hypoxia.

Résumé : Afin d'analyser la relation qui existe entre l'érythropoïèse et le métabolisme du fer, une des questions soulevées dans cette étude consiste à connaitre la biodisponibilité du fer en conditions physiopathologiques. Notre but était de comprendre l'axe fonctionnel de réponse composé de l'érythropoïétine (Epo) – hepcidine – ferroportine (FPN) lorsque deux états dysfonctionnels coexistent, à l'aide d'un modèle animal de surcharge en fer suivie d'une hypoxie. La FPN et la prohepcidine ont été estimées par immunohistochimie à l'aide d'une anticorps polyclonal anti-FPN de souris produit chez le lapin et d'un anticorps monoclonal anti-prohepcidine. Le système Envision+ constitué de polymère marqué à la peroxydase de raifort anti-lapin produit chez la chèvre a été utilisé comme anticorps secondaire. Les niveaux d'Epo ont été mesurés par ELISA. Le fer tissulaire a été étudié par coloration au Bleu de Prusse. L'érythropoïèse a été évaluée par des tests hématologiques conventionnels. La surcharge en fer accroissait la prohepcidine qui demeurait élevée en hypoxie, coexistant avec de hauts niveaux d'Epo en hypoxie, avec ou sans surcharge. En hypoxie, la FPN était clairement évidente dans les macrophages réticulo-endothéliaux, davantage que lors de l'hypoxie avec surcharge en fer. Fait intéressant, la FPN duodénale était clairement détectable dans les membranes basolatérales en hypoxie, avec ou sans surcharge en fer. Nos données indiquent que deux signaux pourraient induire une réponse spécifique au type de cellules : (*i*) le signal du fer, qui a induit la prohepcidine, laquelle réduit la FPN réticulo-endothéliale et conséquemment la disponibilité en fer ; (*ii*) le signal hypoxique qui a stimulé l'Epo, affectant l'absorption du fer en stabilisant la FPN duodénale, permettant un apport en fer pour l'érythropoïèse, indépendamment de la taille des réserves. [Traduit par la Rédaction]

Mots-clés : ferroportine, prohepcidine, érythropoïétine, fer, hypoxie.

Introduction

Iron is an essential nutrient for the growth and development of all living organisms, particularly for mammalian erythropoiesis (Fleming 2008). It is well known that body iron homeostasis is maintained through a balance between iron recycling from senescent erythrocytes within the reticuloendothelial system (RES) and iron absorption from the diet by duodenal enterocytes (Ganz and Nemeth 2006). Two to three million red blood cells (RBCs) are produced every second and require 30–40 mg of iron delivered to the erythron to make 30 pg of hemoglobin (Hb) per cell, a total of 6 g of Hb daily (Li and Ginzburg 2010). The pool of iron bound to transferrin (Tf-Fe(III)) is 10 times smaller than the daily iron requirements, requiring rapid turnaround to ensure sufficient delivery of iron. Daily iron required for erythropoiesis is predominantly derived from recycling of heme iron by macrophages erythrophagocytosing senescent RBCs (Knutson and Wessling-Resnick 2003).

These processes resulted from the combined action of 2 regulators, namely, the store regulator and the erythroid regulator (Finch 1994). The store regulator regulates iron absorption and is responsible for meeting iron requirements and for controlling iron stores. The erythroid regulator transmits erythroid demands irrespective of the body's iron balance (Pak et al. 2006).

Iron metabolism and erythropoiesis are closely linked. Because the majority of iron can be found in the Hb compartment, erythropoiesis dominates iron metabolism (Li and Ginzburg 2010). This dynamic process of iron trafficking for erythropoiesis requires a link to prevent iron deficiency or iron overload. It is well known that erythropoietin (Epo) is the hematopoietic growth factor that stimulates proliferation, differentiation, and survival of erythroid precursor cells (Fandrey 2004). Erythropoiesis depends on iron availability, and in fact, the amount of iron in RBCs is so large that increases in erythropoiesis require a considerable increase in the flow of iron from the diet or storage pools.

Received 26 June 2012. Accepted 13 December 2012.

M.C. D'Anna and M.E. Roque. Laboratory of Human Physiology, Department of Biology, Biochemistry and Pharmacy, San Juan 670, Universidad Nacional del Sur, Bahía Blanca, Argentina.

Corresponding author: Marta E. Roque (e-mail: mroque@uns.edu.ar).

The coordination and regulation of processes related to body iron homeostasis has been ascribed to hepcidin, which has the role as negative regulator of intestinal iron absorption and release from stores (Nicolas et al. 2002). Hepcidin mRNA levels are homeostatically regulated by body iron stores, erythroid iron needs, hypoxia, and inflammation (Viatte and Vaulont 2009). Hepcidin acts by regulating its receptor, ferroportin (FPN), triggering its degradation (Nemeth et al. 2004). The regulation of the iron exporter FPN, expressed in enterocytes and macrophages of the RES, is currently being studied, since both transcriptional and post-transcriptional regulation induce changes in its expression and localization (Abboud and Haile 2000; Delaby et al. 2008; D'Anna et al. 2009). Therefore, in the presence of hepcidin, iron efflux from FPN-expressing cells is greatly decreased. Recently, it has been suggested that the effects of hepcidin could be cell-type specific, and to date, it is not apparent whether the action of hepcidin represents a global mechanism in all FPN-expressing cells (Chaston et al. 2008).

Several physiopathological situations are related to changes in iron-related proteins such as hepcidin and FPN and also in the erythroid response that includes Epo expression. Alteration of erythropoietic activity is an appealing mechanism for the regulation of hepcidin and also regulates the production of Epo (Pak et al. 2006; Vokurka et al. 2006). Experimental iron overload results in iron accumulation in macrophages, and later in hepatocytes, and regulates hepcidin levels as well as FPN expression (Theurl et al. 2005). Therefore, the inter-relationships among Epo, hepcidin, and FPN play a critical role in iron imbalance that characterizes iron disorders such as the anemia of chronic diseases.

The aim of this study was to understand the functional axis response of Epo–hepcidin–FPN when 2 dysfunctional states coexist: (*i*) iron overload and (*ii*) hypoxia. We put special emphasis on proteins regulating iron metabolism and how the stimulus of erythropoietic activity affects their expression. To perform this study we developed an in vivo coupled model as a strategy to study the inter-relationships between erythropoiesis and iron metabolism. Understanding the relations between these proteins will extend our knowledge in the field of iron and erythropoiesis.

Materials and methods

Animals

CF1 female mice (30 ± 5 g; 3 months old) were bred at the animal facility of the Universidad Nacional del Sur. The animals were kept in cages at controlled room temperature and humidity for 10 days prior to the commencement of the study and were fed throughout on a standard diet with access to water ad libitum, under standard conditions (12 h light : 12 h dark). The procedures followed were in line with the Canadian Council on Animal Care guidelines. Prior to the initiation of this study, the protocol was approved by the Institutional Committee on Experimental Animal Use and Care of the Universidad Nacional del Sur.

Experimental design

Adult female mice (CF1) were divided into 4 groups (8 mice per group) following a block design and they were studied for 33 days. The groups of mice were divided as follows: (*i*) basal group receiving saline solution intraperitoneally (i.p.) (0.9% NaCl) on days 0 and 10 and maintained in normoxia from day 21 to day 33; (*ii*) iron overload group (without hypoxia) receiving 1 g Fe-dextran/kg body mass i.p. (Fexiron Rivero Laboratories, Argentina) on days 0 and 10 and maintained in normoxia from day 21 to day 33; (*iii*) hypoxia group (without iron overload) receiving saline solution i.p. (0.9% NaCl) on days 0 and 10 and maintained in hypoxia from day 21 to day 33; and (*iv*) iron overload + hypoxia group receiving 1 g Fe-dextran/kg body mass i.p. on days 0 and 10 and maintained in hypoxia from day 21 to day 33.

For in-vivo hypoxia, mice were housed in a normobaric chamber and exposed to a PiO_2 = 79 mm Hg (1 mm Hg = 133.322 Pa) at normal barometric pressure. We used a certified mixture of gases (8.5% O_2 and 91.5% N_2) (Air Liquide). In the chamber, mice were maintained at an ambient temperature of 22 ± 2 °C with a 12 h light : 12 h dark cycle, and had free access to food and water.

Tissue preparation

A subset of each group of animals (n = 3) were sacrificed by cervical dislocation. The duodenum, spleen, and liver were removed and fixed in 10% buffered formalin. Tissues were embedded in paraffin and 5 μm sections were obtained.

Antibodies

Primary antibodies against mouse FPN were raised against a peptide corresponding to the C-terminus of FPN (GPDEKEVTDENQPNTS), provided by Bruno Galy, of the European Molecular Biology Laboratory, Germany. The characterization of the FPN antibody was developed by McKie et al. (2000) using protein extracts from Hela cells transfected with a mouse FPN cDNA, as reported by Galy et al. (2005). Prohepcidin immunodetection was performed with anti-mouse prohepcidin (Alpha Diagnostic). Goat-labeled polymer – horseradish peroxidase (HRP) anti-rabbit EnVision + System (DAB) (DakoCytomation, Carpinteria, California, USA) was used as the secondary antibody.

Immunohistochemistry

The sections were processed for immunohistochemistry by 3-3′-diaminobenzidine tetrahydrochloride staining. Tissue sections were deparaffinized and dipped in an aqueous 3% solution of hydrogen peroxide for 15 min to inhibit any endogenous peroxidase activity. After washing in PBS (pH 7.0), sections were incubated for 1 h at room temperature with rabbit polyclonal antiserum against mouse FPN and overnight at 4 °C for prohepcidin immunodetection. Dilutions of antibodies were as follows: anti-FPN, diluted 1:500 with PBS (pH 7.0); and anti-prohepcidin, diluted 1:100 with PBS (pH 7.0). After washing, sections were incubated for 30 min with peroxidase-labeled polymer-HRP conjugated to goat anti-rabbit immunoglobulins (EnVision + System-HRP-DAB). Staining was completed by incubation with 3,3′-diaminobenzidine chromogen solution (chromogen solution was part of the Envision kit). The sections were then counterstained with Harris's haematoxylin, dehydrated, and mounted. Negative controls included incubation with PBS without the primary antibody. Immunostaining was analyzed using an Olympus BX51 microscope, equipped with 10×, 20×, and 40× dry objectives and a 100× oil immersion objective. Digital images were acquired with an Olympus C7070 camera.

Prussian blue iron staining

Deparaffinized tissue sections were incubated in 2% HCl containing 10% potassium ferrocyanide for 15 min, washed, and counterstained with nuclear red before visualization. Some of the spleen and liver sections were treated with anti-FPN antibody and anti-prohepcidin antibody using the immunohistochemistry technique followed by Prussian blue iron staining to determine the presence of hemosiderin deposits in FPN-positive cells. These sections were counterstained with nuclear red.

Western blot analysis

Protein was extracted by homogenizing tissues in lysis buffer (50 mmol/L Tris–HCl, 150 mmol/L NaCl, 1 mmol/L EDTA, 1% Tween-20, and 1% Triton X-100) containing protease inhibitor cocktail (Sigma–Aldrich). The homogenate was centrifuged at 10 000*g* for 10 min at 4 °C. The resulting supernatant was used for protein concentration analysis in the Bradford assay. Protein (100 μg) was solubilized in Laemmli loading buffer and separated by SDS–PAGE on 12% gels, transferred onto nitrocellulose membrane, blocked with 5% bovine serum albumin (BSA) in Tris-buffered saline with

0.1% Tween-20 (TBST) for 1 h, and further incubated with rabbit anti-mouse FPN antibody (Alpha Diagnostic, gifted by Marco T. Nuñez, Chile) overnight at 4 °C. As a housekeeping control, we used rabbit anti-mouse GAPDH antibody (Cell Signaling), incubated for 1 h at room temperature. Immunoreactivity was observed using a HRP-linked secondary antibody (Thermo Scientific). Reactions were detected by enhanced chemiluminescence following the manufacturer's directions. Blot densitometry was obtained using ImageJ software.

Hematology

Animals were anesthetized with diethyl ether for blood collection to determine hematological parameters hematocrit (HCT), Hb, and reticulocytes. Epo plasma levels were measured using the Quantikine mouse/rat Epo immunoassay kit (R&D Systems) in accordance with the manufacturer's instructions. For each time point, samples from 4 individual mice from each group were collected from the retro-orbital venous plexus (25 μL each).

Plasma and tissular iron

In plasma samples from mice, iron levels were detected by the colorimetric ferrozine-based assay (Fer Color, Wiener Lab). Liver iron content was determined after acid digestion of hepatic samples followed by iron quantification with the colorimetric ferrozine-based assay.

Statistical analysis

In all mouse experiments, at least 4 mice were tested individually. Data were analyzed by 1-way ANOVA across the 4 groups followed by a Tukey's multiple comparison test. The level of statistical significance was set at $p < 0.05$. All values are expressed as the mean ± SD.

Results

Erythropoiesis study

Hematological data

Values for Hb and reticulocytes are shown in Table 1. Hb values showed a statistically significant rise on day 26 in the iron overload + hypoxia group and in the hypoxia group. These values correlate inversely with Epo levels. Reticulocytes showed a statistically significant rise on day 23 in the iron overload + hypoxia group and in the hypoxia group.

Erythropoietin

Values for plasma Epo are shown in Table 1. When mice were housed in the hypoxia chamber (from day 21 to day 33), we observed a fast and a statistically significant increase of Epo levels 6 h after the beginning of hypoxia (these values were evaluated 6 h after the beginning of hypoxia at day 21). This increase was observed in the iron overload + hypoxia group and in the hypoxia group.

Iron study

Plasma iron levels

The study of plasma iron levels revealed a significant increase in the iron overload + hypoxia group on day 20 of the experimental design (582 ± 78 μg/dL) and remained high in all hypoxia induction compared with values of the basal group (335 ± 61 μg/dL).

Hepatic iron

The study of hepatic iron showed a significant increase in the iron overload + hypoxia group from day 0 (14 ± 9 μmol/g dry tissue) to day 20 (2000 ± 290 μmol/g dry tissue), remaining high in all hypoxia induction (from day 21 to day 33). Iron dextran treatment increased hepatic hemosiderin that localized not only in Kupffer cells but also in some hepatocytes (Figs. 1C and 1D).

Table 1. Erythropoietin levels and hematological data in the control group, iron overload group, hypoxic group, and hypoxia with iron overload group throughout the experimental protocol (day 0–33).

	Control group			Iron overload group			Hypoxia group			Iron overload + hypoxia group		
	Hematological data			Hematological data			Hematological data			Hematological data		
Day	Hb (g/dL)	Reticulocytes (%)	Epo (pg/dL)	Hb (g/dL)	Reticulocytes (%)	Epo (pg/dL)	Hb (g/dL)	Reticulocytes (%)	Epo (pg/dL)	Hb (g/dL)	Reticulocytes (%)	Epo (pg/dL)
0	14.3±0.6	2.8±0.4	137±25	14.6±0.3	2.6±0.3	162±31	14.5±0.9	3.2±0.9	178±60	14.1±0.5	2.5±0.3	155±63
20	15.1±0.9	2.8±0.6	173±43	13.8±0.3	2.0±0.6	145±28	14.7±0.3	2.8±0.4	255±114	13.6±0.4	2.2±0.4	225±85
21 (6 h)	14.4±0.2	2.2±0.4	174±60	13.4±0.5	2.5±0.3	220±58	14.3±0.4*,††	2.1±0.2	3261±288†,††	12.6±0.3	2.7±0.9	2993±473†,††
23	14.9±0.3	3.0±0.9	223±63	13.4±0.3	3.7±0.9	312±28	15.6±0.5*,††	8.4±0.4**,***	582±344**,***	14.3±0.5	8.1±1.6**,***	478±241**,***
26	14.9±0.2	2.3±0.7	306±43	13.9±0.2	2.4±0.5	203±59	16.9±0.6**,***	5.6±1.6	754±533**,***	15.8±0.5**,***	5.1±0.6	716±517**,***
29	14.1±0.8	2.6±0.5	240±85	13.7±0.7	2.9±0.5	281±76	17.4±0.5**,***	5.3±1.6	262±145	16.3±0.4**,***	2.9±1.1	355±114
33	14.3±0.7	2.9±0.9	194±25	13.8±0.4	3.4±0.7	177±30	17.8±0.8**,***	5.0±0.3	208±39	16.4±0.7**,***	5.1±2.2	359±56

Note: Hypoxia began on day 21 for the hypoxia group and for the iron overload + hypoxia group. Values for hemoglobin (Hb), reticulocytes, and erythropoietin (Epo) of the iron overload group and control group did not change throughout the experimental protocol. Values are the mean ± SD ($n = 4$); *, $p < 0.05$ vs. the iron overload + hypoxia group; **, $p < 0.05$ vs. the iron overload group; ***, $p < 0.05$ vs. the control group; †, $p < 0.01$ vs. the iron overload group; ††, $p < 0.01$ vs. the control group.

Fig. 1. Immunolocalization of hepatic prohepcidin. (A) Hepatic tissue of basal condition group showing expression in hepatocytes near blood vessels (arrow indicates brown staining). (B) Hepatic tissue of basal condition group showing intracellular localization in hepatocytes near blood vessels (arrow indicates brown (Web site only) staining). (C) Hepatic tissue of iron overload group showing high cytoplasmic expression (arrow indicates brown staining) and hemosiderin (blue (Web site only) staining). (D) Hepatocytes of iron overload group showing high cytoplasmic expression (arrow indicates brown staining) and hemosiderin in Kupffer cells and hepatocytes (blue staining). (E) Hepatic tissue of hypoxia group showing low expression in hepatocytes (brown staining). (F) Hepatocytes of hypoxia group showing expression in hepatocytes (brown staining). (G) Hepatic tissue of iron overload + hypoxia group showing high cytoplasmic expression (arrow indicates brown staining) and hemosiderin (blue staining). (H) Hepatocytes of iron overload + hypoxia group showing high cytoplasmic expression (arrow indicates brown staining) and hemosiderin (blue staining). (I and J) Negative controls of liver. Liver sections were prepared as described in the Materials and methods. The time point represented is day 26. BV, blood vessel. Scale bars = 20 μm.

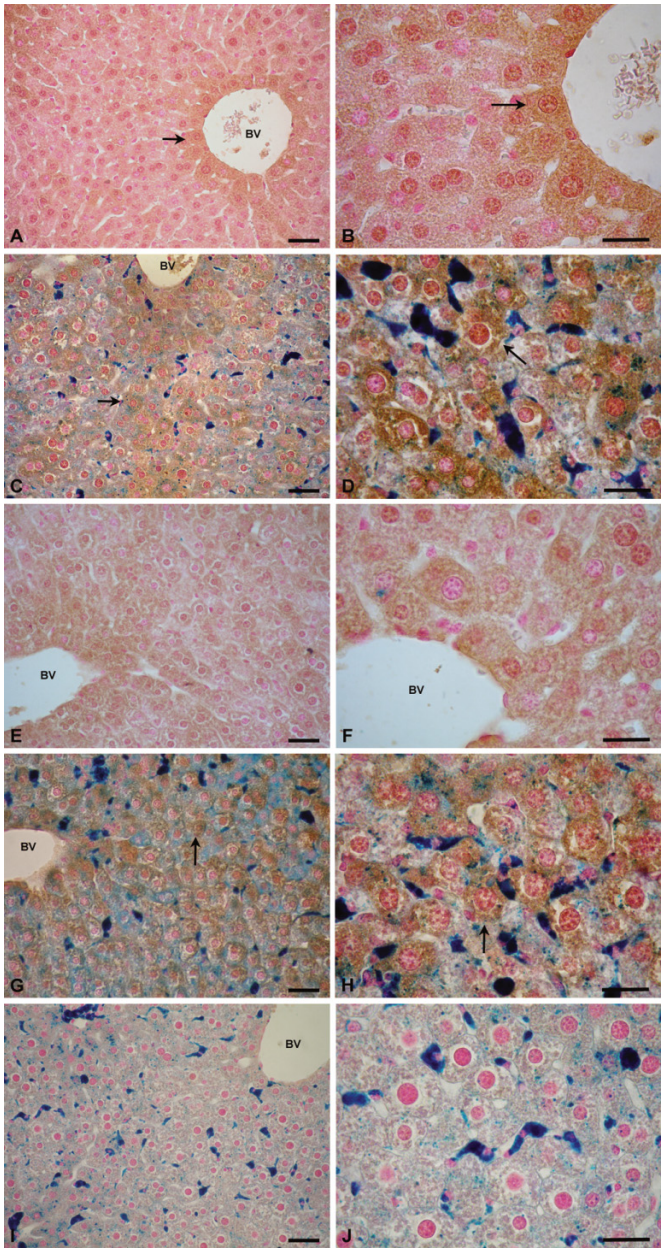

Iron proteins study

Hepatic prohepcidin expression

Hepatic lobules of the basal group were heterogeneous with respect to prohepcidin immunoreactivity. Within a hepatic lobule, prohepcidin expression was predominantly located in hepatocytes associated with central veins, with only a few positive hepatocytes in periportal zones (Figs. 1A and 1B). In the iron overload group, prohepcidin expression was particularly marked in hepatocytes including expression near blood vessels. Kupffer cells and endothelial cells lacked of prohepcidin immunoreactivity (Figs. 1C and 1D). A dramatic increase in iron deposits were seen not only in Kupffer cells but also in hepatocytes (Figs. 1C and 1D). In the hypoxia group, prohepcidin expression decreased, noting a few hepatocytes near blood vessels positive for this propeptide (Figs. 1E and 1F). Interestingly, in the iron overload + hypoxia group, prohepcidin expression remained clearly identified in hepatocytes (Figs. 1G and 1H).

Ferroportin expression

Splenic macrophages

Splenic FPN expression in the basal group was evident in red pulp macrophages surrounding nodules of white pulp, without FPN expression in the white pulp (Fig. 2A). Immunoreactivity in the red pulp was observed both cytoplasmically and on the plasma membrane of macrophages. By means of the double-staining method, in red pulp we were able to observe a large number of macrophages stained for FPN that also had hemosiderin.

Splenic macrophages of the iron overload group showed negative FPN immunostaining and were positive for hemosiderin compared with the basal group (Fig. 2B). In the hypoxia group, we observed a clearly identified and particularly marked FPN expression in red pulp macrophages (Fig. 2C). However, in the iron overload + hypoxia group, FPN expression was less evident in red pulp macrophages; this pattern was similar to that observed in the iron overload group (Fig. 2D). This pattern of FPN expression was seen from day 23 of hypoxia to day 33. The time point represented in Fig. 2 is day 26.

Immunohistochemical studies of FPN expression in spleen were useful to show the distribution and activity of FPN in this tissue. Studies of splenic FPN expression done by Western blot analysis were consistent and confirmed our results observed by immunohistochemistry (Fig. 3A).

Kupffer cells

FPN expression in the liver of the basal group was limited to a few cells identified as Kupffer cells on the basis of their cell morphology, where expression was found to be cytoplasmic and also at the plasma membrane (Fig. 2E).

Iron overload resulted in downregulation of FPN expression, as only a few discrete Kupffer cells were positive for FPN (Fig. 2F). In the hypoxia group, we observed a marked FPN expression that was clearly identified in the cell membrane of Kupffer cells (Fig. 2G).

However, in the iron overload + hypoxia group, FPN expression was less evident in Kupffer cells, this pattern was similar to that seen in the iron overload group (Fig. 2H). This pattern of expression was seen from day 23 of hypoxia to day 33. The time point represented in Fig. 2 is day 26.

Immunohistochemical studies of FPN expression in liver were useful to show the distribution and activity of FPN in this tissue. Studies of hepatic FPN expression done by Western blot analysis revealed the level of expression in this tissue in all conditions studied (Fig. 3B).

Fig. 2. Ferroportin (FPN) expression in spleen, liver, and duodenum. (A) Splenic tissue of healthy mice showing FPN on macrophages of the red pulp and colocalization with hemosiderin (arrow). (B) Red pulp of iron overloaded mice showing lack of FPN and hemosiderin (blue, Web site only) on macrophages. (C) Red pulp of hypoxic mice showing marked FPN expression and hemosiderin (blue) on macrophages (arrow). (D) Red pulp of iron overloaded mice with hypoxia showing lack of FPN and hemosiderin (blue) on macrophages. (E) Hepatic tissue of healthy mice showing FPN on Kupffer cells (arrow). (F) Hepatic tissue of iron overloaded mice showing lack of FPN expression. (G) Hepatic tissue of hypoxic mice showing marked FPN expression on Kupffer cells (arrow). (H) Hepatic tissue of iron overloaded mice with hypoxia showing lack of FPN and hemosiderin (blue) on Kupffer cells. (I) Duodenum of healthy mice showing supranuclear and slight basolateral FPN expression (arrow). (J) Duodenum of iron overloaded mice showing supranuclear FPN expression (arrow). (K) Duodenum of hypoxic mice showing high intracellular and basolateral FPN expression (arrow). (L) Duodenum of iron overloaded mice with hypoxia showing both intracellular and basolateral FPN expression in enterocytes. Negative controls of (M) spleen, (N) liver, and (O) duodenum. Tissue sections were processed as described in the Materials and methods. The time point represented is day 26. RP, red pulp; WP, white pulp. Scale bars represent 20 μm.

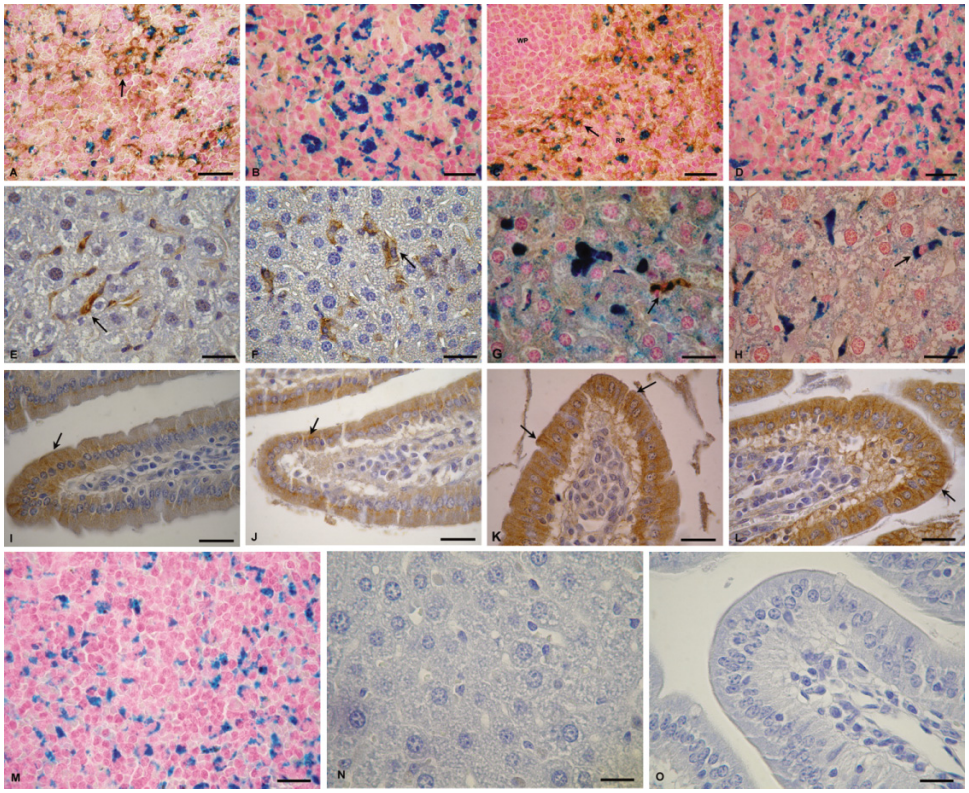

Fig. 3. Expression of ferroportin (FPN) in spleen, liver, and duodenum by Western blot analyses. The sizes (in kDa) of FPN and GAPDH are indicated on the right. Immunoblotting analysis of (A) splenic FPN, (B) hepatic FPN, and (C) duodenum FPN. a, control; b, iron overload; c, hypoxia; and d, iron overload + hypoxia. The time point represented is day 26 ($n = 3$); *, $p < 0.05$ (control vs. each experimental group); #, $p < 0.05$ (hypoxia vs. iron overload + hypoxia).

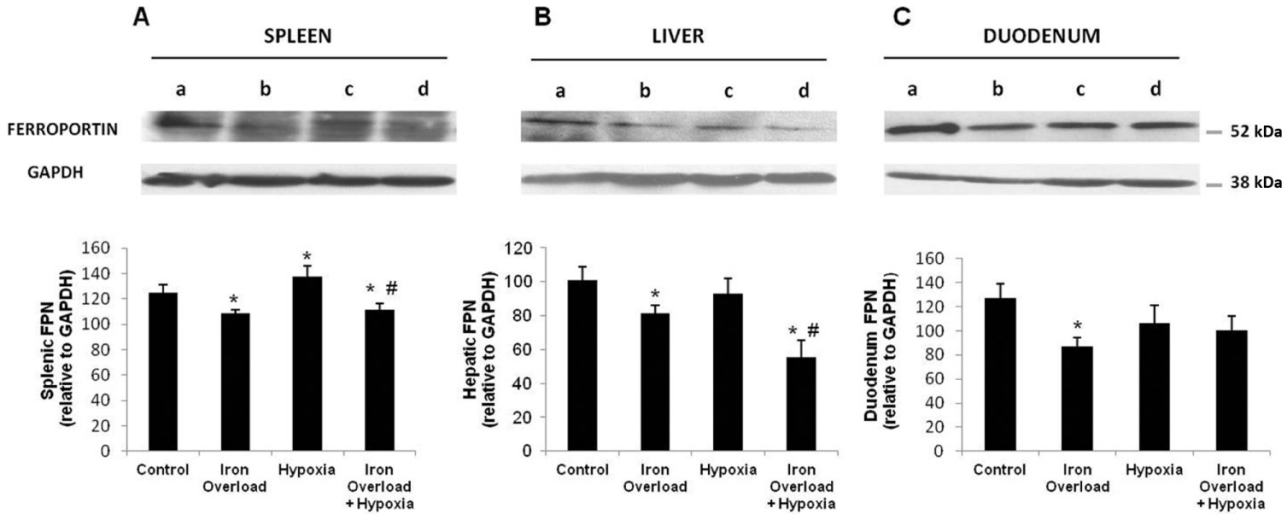

Duodenal enterocytes

In the basal group, FPN was detected mainly inside enterocytes, localized immediately above the nucleus on the apical side, with slight basolateral expression (Fig. 2I). This pattern of expression was also observed after iron overload treatment, but without basolateral FPN expression (Fig. 2J). In the hypoxia group, we observed a dramatic increase in FPN expression along the basolateral surface of duodenal enterocytes and cytoplasmatically (Fig. 2K).

Interestingly, duodenal FPN expression in the iron overload + hypoxia group showed the same pattern of distribution that was observed in the hypoxia group. We could observe not only intracellular FPN expression but also a redistribution along the basolateral membrane throughout villous enterocytes (Fig. 2L). This pattern of expression was seen from day 23 of hypoxia to day 33. The time point represented in Fig. 2 is day 26.

Immunohistochemical studies of FPN expression in duodenal enterocytes were useful to show the distribution of FPN in this tissue. Studies of duodenal FPN expression done by Western blot analysis revealed the level of expression in this tissue in all conditions studied (Fig. 3C).

Although duodenal FPN expression in the iron overload + hypoxia group showed the same pattern of expression that was observed in the hypoxia group, duodenal FPN levels in the control group seem to be higher than those observed in the hypoxia group.

Discussion

To analyze the interconnection between erythropoiesis and iron metabolism, one of the issues raised in this study was to know iron bioavailability in cells under different physiopathological conditions. Therefore, we intended to design a coupled animal model where 2 physiopathological stimuli, such as iron overload and hypoxia, coexist. The idea behind this new approach was to induce 2 dysfunctional states on iron bioavailability in cells, which is strictly related with the iron exporter FPN. In this sense, the main purpose was to increase our knowledge about the relation between erythropoiesis and the iron cycle, studying the functional axis composed of Epo—hepcidin–FPN.

The physiological mechanisms that are triggered by hypoxia showed Epo-dependent active erythropoiesis. Indeed, under hypoxia conditions with and without iron excess, the renal response to low PO_2 was represented by an early and sharp increase in plasma Epo, which showed that the system regulating erythropoiesis was working properly. It is worth mentioning that the inverse relationship between Epo and Hb responded to a temporary profile as described in human beings in iron deficiency anemia (Roque et al. 2001). This Epo–Hb functional relationship coincides with the molecular events responsible for the differentiation of Epo-dependent erythroid progenitors (Fandrey 2004).

Splenic and hepatic FPN in hypoxia with iron excess showed a typical expression profile of the inhibitory effects of hepcidin. From our results, we may conclude that the physiological mechanisms induced by hypoxia, with iron sufficiency, produce a quick release of this nutrient since they occur with a noticeable FPN expression on the cell membrane, especially in red pulp macrophages and Kupffer cells. However, in iron overload + hypoxia, the regulatory mechanisms involved in the hypoxic response prevent the release of iron through the action of FPN. We suggest that iron excess prevails over the hypoxic stimulus because of the decrease in splenic and hepatic FPN, which was caused by the inhibitory effect of hepcidin on this exporter. The reduction of FPN in the plasma membrane of macrophages in spleen and liver could reduce iron bioavailability, increasing its accumulation. This reduction of FPN activity and the less evident localization on the cell membrane observed by immunohistochemical studies was consistent with the Western blot analysis, which revealed a lower quantity of splenic and hepatic FPN in hypoxia with iron excess.

Based on our results of duodenal FPN in hypoxia with iron excess, we demonstrated that in this tissue there was an exporter expression profile similar to that observed in hypoxia without iron excess. The evident increase in intracellular expression and the redistribution of duodenal FPN to the basolateral membrane of enterocytes suggest an active transfer of iron into the bloodstream, even when there is iron overload. To explain why duodenal FPN expression increases in hypoxia, even with iron excess, an interesting hypothesis we postulated is that Epo has a regulatory function mainly on duodenal FPN. Therefore, Epo could stimulate erythropoiesis in response to hypoxia, regardless of iron balance, influencing both FPN and hepcidin expression. Our hypothesis of a direct role of Epo on FPN expression in duodenum is actually in line with a recent study by Liu et al (2012). In this study they found that hypoxia inducible factor (HIF)-mediated suppression of the hepcidin gene required Epo induction and was associated with elevated serum growth differentiation factor 15 (Gdf15). Additionally, there is evidence that increased HIF-α activity causes suppression of hepcidin and increased FPN levels (Peyssonnaux et al. 2007; Lee and Beutler 2009). Recently, it has been shown that the FPN promoter contains HIF-responsive elements (HRE) and HIF-2α directly binds to the FPN promoter, inducing its expression (Taylor et al. 2011). Therefore, this could support our hypothesis that the Epo–HIF axis and additional erythroid mediators (such as Gdf15 and Tmprss6) could be related in regulating not only FPN expression in duodenum in hypoxia even with iron excess, but also hepcidin.

Recent studies also support our results through the identification of an alternative upstream promoter to express a FPN transcript, the isoform B of FPN, which lacks iron responsive elements and is not repressed under iron-deficient conditions (Zhang et al. 2009; Cianetti et al. 2010). Isoform B in enterocytes could act by exporting iron independently from the iron regulatory protein – iron responsive element system, even with iron overload. Based on the above, we suggest that the isoform B of FPN in enterocytes allows an active iron export to the bloodstream to meet systemic iron demands in hypoxia with iron excess.

Therefore, we suggest that many factors, such as HIFs, reactive oxygen species, erythroid factors, and FPN isoforms, could be related to FPN expression in duodenum.

Another point that needs clarification is the high levels of duodenal FPN expression seen in the basal conditions, compared with the hypoxia with and without iron groups. This difference in terms of quantity could be that in basal conditions FPN expression is not only in intracellular compartments but also on the cell membrane. In hypoxia with and without iron, FPN is concentrated on the cell membrane and apparently its levels are less but enough to be part of active iron exportation.

In enterocytes, FPN could be part of the signaling pathway through which erythron communicates iron needs to expand the erythroid compartment in hypoxia, regardless of systemic iron (Li and Ginzburg 2010). This is an interesting observation, for it connects iron uptake from the diet with erythropoiesis, despite iron overload in stores.

Given that macrophages recycle 20–30 mg of iron per day from senescent erythrocytes compared with the 1–2 mg of iron a day that is absorbed by enterocytes, this regulation pattern is fully consistent with the relative contributions of these 2 cell types to maintain body iron homeostasis (Chung et al. 2009). Therefore, to reduce iron bioavailability, the reduction of the iron exporter FPN through hepcidin interaction in hypoxia with iron overload is particularly important and evident in macrophages. We would like to emphasize that the presence of alternative FPN transcripts without iron responsive elements in enterocytes may make any alterations in FPN mRNA splicing relevant under pathological

Fig. 4. Diagram of the prohepcidin, erythropoietin, and ferroportin axis in (A) iron overload, (B) hypoxia, and (C) iron overload + hypoxia.

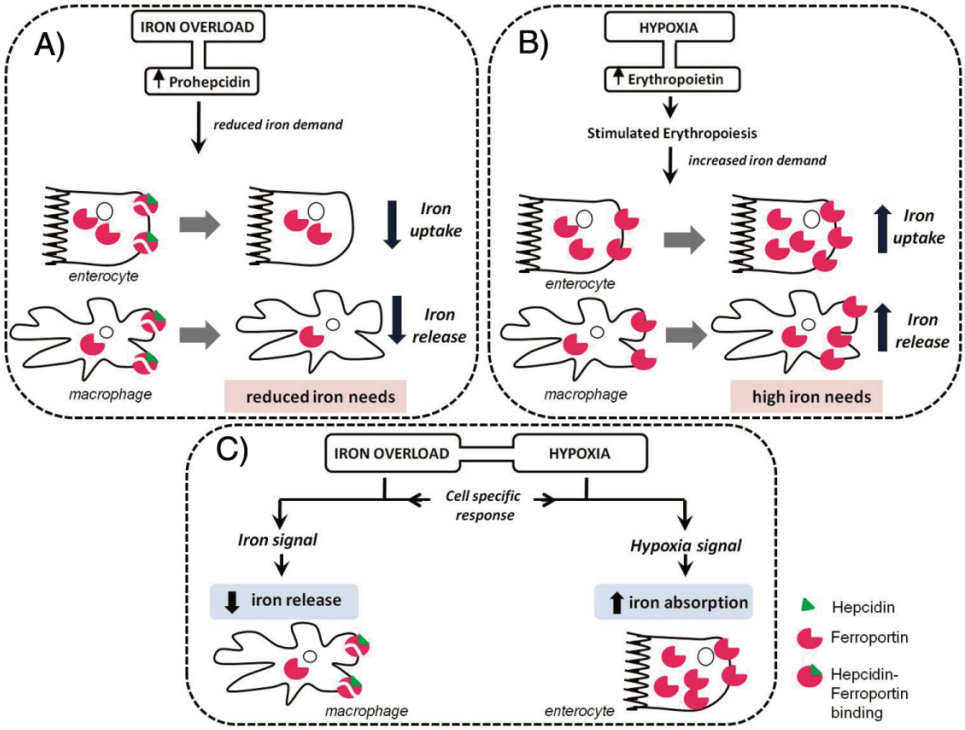

conditions related to the iron cycle. Thus, FPN expression in enterocytes in hypoxia, even with iron overload, could be explained by FPN isoforms. However, at the moment we are unable to confirm this behavior since it is hard to find specific antibodies in the market. Therefore, further studies will be required to identify what FPN isoforms are regulating iron exportation in hypoxia with iron overload and how these isoforms are regulated by hepcidin.

In view of the proposed FPN regulation, it is worth noting the importance of evaluating the expression profile of prohepcidin when both iron excess and hypoxia are present. Indeed, we demonstrated that the prohepcidin regulatory response depended on the systemic and local needs of iron and that its expression in iron overload remained high in hypoxia. In other words, in our coupled model, the signal that prevailed over prohepcidin synthesis was the iron excess signal rather than the hypoxic–Epo dependent signal.

The coexistence of high levels of prohepcidin and Epo in hypoxia with iron excess allows us to analyze another issue raised in our study. The strategy of the coupled design allowed us to study in the Epo–hepcidin–FPN axis whether the erythropoietic hormone, i.e., Epo, could stimulate erythropoiesis and at the same time inhibit hepcidin.

We based the analysis of hepcidin and Epo to take into account their differential distribution and the specific function of each protein. With regard to this, the role of hepcidin in iron overload would be to prevent intestinal absorption and iron release from the RES mediated by FPN. Epo would respond to hypoxia by increasing erythropoiesis, a process that in turn, would depend on iron bioavailability. Our results showed that both proteins, Prohepcidin and Epo, responded independently from the stimuli presented: iron excess and hypoxia, respectively.

With regard to the hepcidin regulatory model, it should be noted that in our coupled model there was enough iron available for erythropoiesis induced by hypoxia, since an adequate regenerative response was evidenced by reticulocytosis in hypoxia with iron excess. Hence, the sustained prohepcidin expression in hypoxia with iron excess reduced iron availability in liver and spleen, but surprisingly not in duodenum. In duodenum, the strong intracellular and basolateral FPN expression allowed iron uptake from diet for erythropoiesis in hypoxia.

Finally, we may conclude that 2 pathways of signals could induce the cell-specific response observed (Fig. 4) as follows: (*i*) iron signal, induced prohepcidin synthesis, which reduced the activity of reticuloendothelial FPN, reducing iron availability; and (*ii*) hypoxia signal, stimulated Epo, which affected iron absorption by stabilizing duodenal FPN and, therefore, allowed iron supply to the bone marrow, regardless of high iron stores. In conclusion, the interplay between Epo and key proteins of the iron cycle, such as hepcidin and FPN, may help to better understand the mechanisms involved in iron and erythropoiesis regulation.

Acknowledgements

This research was supported by the Secretaría General de Ciencia y Tecnología de la Universidad Nacional del Sur (Grant 24/B116) and the Agencia de Promoción Científica y Tecnológica (FONCYT) (Grant-908). We thank Dr. Matthias Hentze, Dr. Bruno Galy, and Dr. Marco T. Nuñez for generously providing FPN antibody reagents. We are very grateful to Dr. Alejandro Curino and all his lab members.

References

Abboud, S., and Haile, D.J. 2000. A novel mammalian iron-regulated protein involved in intracellular iron metabolism. J. Biol. Chem. **275**: 19906–19912. doi:10.1074.jbc.M000713200. PMID:10747949.

Chaston, T., Chung, B.M., Mascarenhas, M., Marks, J., Patel, B., Srai, S.K., et al. 2008. Evidence for differential effects of hepcidin in macrophages and intestinal epithelial cells. Gut, **57**: 374–382. doi:10.1136/gut.2007.131722. PMID: 17965061.

Chung, B., Chaston, T., Marks, J., Srai, S.K., and Sharp, P.A. 2009. Hepcidin decreases iron transporter expression in vivo in mouse duodenum and spleen and in vitro in THP-1 macrophages and intestinal Caco-2 cells. J. Nutr. **139**(8): 1457–1462. doi:10.3945/jn.108.102905. PMID:19549758.

Cianetti, L., Gabbianelli, M., and Sposi, N.M. 2010. Ferroportin and erythroid cells: an update. Adv. Hematol. **2010**: ID 404173, 12 pages. doi:10.1155/2010/404173. PMID:20827391.

D'Anna, M.C., Veuthey, T.V., and Roque, M.E. 2009. Immunolocalization of Ferroportin in healthy and anemic mice. J. Histochem. Cytochem. **57**(1): 9–16. doi:10.1369/jhc.2008.951616. PMID:18796409.

Delaby, C., Pilard, N., Puy, H., and Canonne-Hergaux, F. 2008. Sequential regulation of ferroportin expression after erythrophagocytosis in murine macrophages: early mRNA induction by haem, followed by iron-dependent protein expression. Biochem. J. **411**(1): 123–131. doi:10.1042/BJ20071474. PMID:18072938.

Fandrey, F. 2004. Oxygen-dependent and tissue-specific regulation of erythropoietin gene expression. Am. J. Physiol. Regul. Integr. Comp. Physiol. **286**(6): R977–R988. doi:10.1152/ajpregu.00577.2003. PMID:15142852.

Finch, C. 1994. Regulators of iron balance in humans. Blood, **84**(6): 1697–1702. PMID:8080980.

Fleming, M.D. 2008. The regulation of hepcidin and its effects on systemic and cellular iron metabolism. Hematology Am. Soc. Hematol. Educ. Program, 151–158. doi:10.1182/asheducation-2008.1.151. PMID: 19074074.

Galy, B., Ferring, D., Minana, B., Bell, O., Heinz, G.J., Muckenthaler, M., et al. 2005. Altered body iron distribution and microcytosis in mice deficient in iron regulatory protein 2 (IRP2). Blood, **106**(7): 2580–2589. doi:10.1182/blood-2005-04-1365. PMID:15956281.

Ganz, T., and Nemeth, E. 2006. Regulation of iron acquisition and iron distribution in mammals. Biochim. Biophys. Acta, **1763**(7): 690–699. doi:10.1016/j.bbamcr.2006.03.014. PMID:16790283.

Knutson, M.D., and Wessling-Resnick, M. 2003. Iron metabolism in the reticuloendothelial system. Crit. Rev. Biochem. Mol. Biol. **38**(1): 61–88. doi:10.1080/713609210. PMID:12641343.

Lee, P.L., and Beutler, E. 2009. Regulation of hepcidin and iron-overload disease. Annu. Rev. Pathol. **4**: 489–515. doi:10.1146/annurev.pathol.4.110807.092205. PMID:19400694.

Li, H., and Ginzburg, Y.Z. 2010. Crosstalk between iron metabolism and erythropoiesis. Adv Hematol. **2010**: ID 605435. doi:10.1155/2010/605435. PMID: 20631898.

Liu, Q., Davidoff, O., Niss, K., and Haase, VH. 2012. Hypoxia-inducible factor regulates hepcidin via erythropoietin-induced erythropoiesis. J. Clin. Invest. **122**(12): 1–10. doi:10.1172/JCI63924. PMID:23114598.

McKie, A.T., Marciani, P., Rolfs, A., Brennan, K., Wehr, K., Barrow, D., et al. 2000. A novel duodenal iron-regulated transporter, IREG1, implicated in the basolateral transfer of iron to the circulation. Mol. Cell, **5**(2): 299–309. doi:10.1016/S1097-2765(00)80425-6. PMID:10882071.

Nemeth, E., Tuttle, M.S., Powelson, J., Vaughn, M.B., Donovan, A., Ward, D.M., et al. 2004. Hepcidin regulates cellular iron efflux by binding to ferroportin and inducing its internalization. Science, **306**(5704): 2090–2093. doi:10.1126/science.1104742. PMID:15514116.

Nicolas, G., Chauvet, C., Viatte, L., Danan, J.L., Bigard, X., Devaux, I., et al. 2002. The gene encoding the iron regulatory peptide hepcidin is regulated by anemia, hypoxia and inflammation. J. Clin. Invest. **110**(7): 1037–1044. doi:10.1172/JCI200215686. PMID:12370282.

Pak, M., Lopez, M.A., Gabayan, V., Ganz, T., and Rivera, S. 2006. Suppression of hepcidin during anemia requires erythropoietic activity. Blood, **108**(12): 3730–3735. doi:10.1182/blood-2006-06-028787. PMID:16882706.

Peyssonnaux, C., Zinkernagel, A.S., Schuepbach, R.A., Rankin, E., Vaulont, S., Haase, V.H., et al. 2007. Regulation of iron homeostasis by the hypoxia-inducible transcription factors (HIFs). J. Clin. Invest. **117**(7): 1926–1932. doi:10.1172/JCI31370. PMID:17557118.

Roque, M.E., Sandoval, M.J., and Aggio, M.C. 2001. Serum erythropoietin and its relation with soluble transferrin receptor in patients with different types of anaemia in a locally defined reference population. Clin. Lab. Haematol. **23**(5): 291–295. doi:10.1046/j.1365-2257.2001.00413.x. PMID:11703410.

Taylor, M., Qu, A., Anderson, E.R., Matsubara, T., Martin, A., Gonzalez, F.J., et al. 2011. Hypoxia-inducible factor-2α mediates the adaptive increase of intestinal ferroportin during iron deficiency in mice. Gastroenterology, **140**(7): 2044–2055. doi:10.1053/j.gastro.2011.03.007. PMID:21419768.

Theurl, I., Ludwiczek, S., Eller, P., Seifert, M., Artner, E., Brunner, P., et al. 2005. Pathways for the regulation of body iron homeostasis in response to experimental iron overload. J. Hepatol. **43**(4): 711–719. doi:10.1016/j.jhep.2005.03.030. PMID:16083989.

Viatte, L., and Vaulont, S. 2009. Hepcidin, the iron watcher. Biochimie, **91**(10): 1223–1228. doi:10.1016/j.biochi.2009.06.012. PMID:19555735.

Vokurka, M., Krijt, J., Sulc, K., and Necas, E. 2006. Hepcidin mRNA levels in mouse liver respond to inhibition of erythropoiesis. Physiol. Res. **55**(6): 667–674. PMID:16497104.

Zhang, D.L., Hughes, R.M., Ollivierre-Wilson, H., Ghosh, M.C., and Rouault, T.A. 2009. A ferroportin transcript that lacks an iron-responsive element enables duodenal and erythroid precursor cells to evade translational repression. Cell Metab. **9**(5): 461–473. doi:10.1016/j.cmet.2009.03.006. PMID:19416716.